

## Experiments in Robotic Boat Localization

Amit Dhariwal and Gaurav S. Sukhatme  
Department of Computer Science, University of Southern California,  
Los Angeles, California, USA  
{dhariwal, gaurav}@usc.edu

**Abstract**—We are motivated by the prospect of automating microbial observing systems. To this end we have designed and built a robotic boat as part of a sensor network for monitoring aquatic environments. In this paper, we describe a dynamic model of the boat, an algorithm for estimating its location by integrating various sensor inputs, a controller for waypoint following and extensive field experiments (over 10 km aggregate) to validate each of these. We test the localization accuracy in different sensing regimes as a prelude to accommodating sensing failures.

### I. INTRODUCTION

The microbiology of aquatic environments is of scientific interest [1]. Its characterization affects our understanding of aquatic food webs, and the impact of urbanization and pollution. It also ultimately plays a role in setting public policy (e.g. regulations on dumping), and other decision making (e.g. when is a beach closure necessary because the water is contaminated?).

Aquatic environmental monitoring has traditionally been done by a human operator performing the sampling manually. This process is inherently slow, tedious, and expensive. To alleviate this, our work is aimed at developing a sensor network to monitor aquatic environments. Our network is composed of static, anchored buoys, and a robotic boat (henceforth 'the boat') all of which communicate with each other. Simply put, the static nodes provide excellent temporal sampling resolution but a limited spatial resolution. The boat is able to traverse the water surface providing high spatial resolution of the data collected but limited temporal resolution. The overall system NAMOS (Networked Aquatic Microbial Observing System) is described in [2], [3] and is extensively documented at <http://robotics.usc.edu/namos>. The project website also contains the biological data collected over the course of several weeks of field experiments during which the boat traveled in excess of 10 km aggregate. The focus of this paper is on the development of a dynamic model of the boat, an algorithm for estimating its location by integrating sensor inputs, a controller for waypoint following and extensive field experiments to validate each of these.

The interplay of ocean currents, waves and wind and their combined effect on watercraft is difficult to model and compensate. Even a seemingly simple action, like station keeping for a boat, can be very difficult. Navigation in such an environment is equally difficult. Imagine driving a bicycle on a suspended rope bridge, with the bridge swaying due

to wind as well as moving due to your changing position. Inherent in their nature, both waves and wind vary over time both in speed and direction in a complex manner. This makes it difficult to compensate for them without having accurate and reliable sensors on board the boat. *Marine* vessel control is an extensively deliberated problem [4]–[6]. Most research in this area has been driven by the requirements of marine applications including off-shore drilling, fisheries and transportation of goods and people. Work on off shore drilling platforms and ships require sea keeping or maintaining position in the presence of wind and water disturbances. Most marine systems use underwater propulsion. The requirements of application warrant the use of an air propeller so as to minimize the disturbance to surface water (which we are trying to sample). Thus our prototype boat is the air-boat shown in Figure 1.

Surface aquatic applications like the one considered here, require only three degrees of freedom to be considered. These are: the motion along the longitudinal axis (surge), translational axis (sway) and rotation along the z axis (yaw or heading) as shown in Figure 4. It is sufficient to accurately and reliably estimate the position (latitude and longitude) and orientation (heading or yaw) of the boat to keep it on track and reach its target locations.

Mobile robot localization is a widely studied problem. However a majority of the work has been focused on land-based robots [7]–[11] and more recently on aerial vehicles [12], [13] and underwater systems [14], [15]. For watercraft, most prior work is for large marine vessels [4]–[6] which mostly deals with dynamic positioning (sea keeping) and steering or maneuvering i.e., ship motion without wave action.

**Contributions:** We describe a dynamic model of the boat, an algorithm for estimating its location by integrating sensor inputs, a controller for waypoint following and extensive field experiments (over 10 km aggregate) to validate each of these. Specifically, we test the localization accuracy in different sensing regimes as a prelude to accommodating sensing failures.

### II. SYSTEM DESCRIPTION

The boat used for testing is a modified radio controlled airboat designed to perform surface sampling (chlorophyll and temperature) at locations of interest. An airboat was chosen as it provides minimal disturbance to the water surface while moving by reducing surface water mixing. We chose a



Fig. 1. Robotic Boat

split hull boat design since two pontoons make for a stable configuration. The boat is equipped with a commercial off-the-shelf GPS (Garmin 16A) and compass (Honeywell HMR 3000) (Figure 2). Both the GPS and compass output NMEA strings at configurable data rates making them ideal for use in our application. We use wind direction and speed sensors from Texas Electronics. See Table I for details on typical sensor characteristics. An Intel X-Scale Stargate processor (PXA 255, 400MHz), is the main processor on the boat. It was selected because of its relatively small form factor, good performance and low power consumption characteristics. Its small size makes it easy to fit it inside the relatively small space available on the boat. It also provides an 802.11b-based wireless link which is used by the boat to transmit and receive data in real time. The navigation hardware on the boat consists of an air propeller and a custom-built rudder which are controlled by a basic stamp module (Parallax BS2sx).

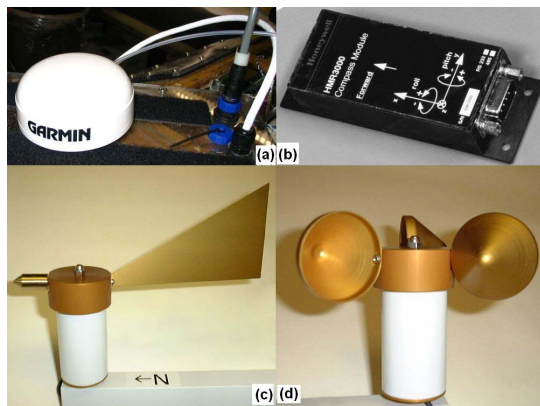


Fig. 2. Sensors. (a) GPS, (b) Compass, (c) Wind direction and (d) Wind speed

The boat monitors two aspects of its environment - the temperature (via a thermistor) and the relative chlorophyll-A concentration (via a CYCLOPS-7 submersible fluorometer from Turner Designs Inc.). The output from these is digitized onboard via a 16 bit ADC. These two sensors are suspended

TABLE I  
TYPICAL SENSOR CHARACTERISTICS. FROM INSTRUMENT MANUALS  
PROVIDED BY MANUFACTURER

Method	Sensor	Obs.	Accuracy	Update Rate
Positioning	Garmin 16A GPS	$x, y$	$< 15m$ (Raw) $3 - 5m$ (with DGPS Correction)	1Hz
Heading (Compass)	Honeywell HMR 3000	$\psi$	$0.5^\circ$	13.75Hz
Wind speed	Texas Electronics TV-4 Sensor	$v_w$	$\pm 0.89m/s$	1Hz
Wind direction	Texas Electronics TD-4 Sensor	$\gamma_w$	$\pm 3^\circ$	1Hz

into the water from the side of the boat (Figure 3). The boat also has a custom built 6 port water sampling system which can collect water samples for lab analysis at specified GPS locations. The boat is powered using rechargeable NiMH batteries and can run for 4-6 hours without recharging.

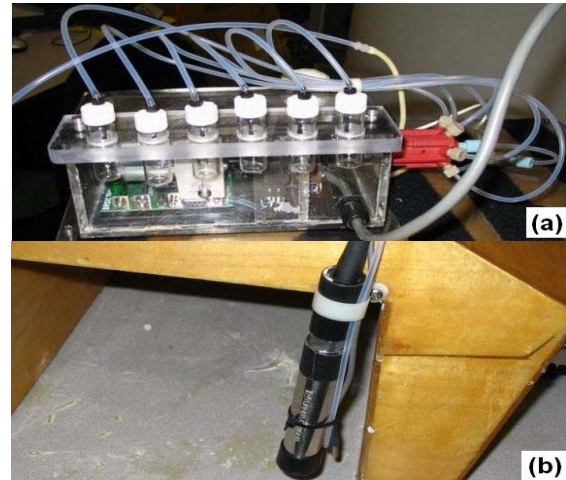


Fig. 3. Environmental sensors on the boat. (a) Water sampler, and (b) fluorometer and thermistor

### III. SYSTEM MODEL

For aquatic applications involving boats and ships, only three degrees of freedom are practically important [5], [16]. These lie in the plane parallel to the surface of the water, namely surge, sway and yaw (Figure 4). It is based upon the fact that the boat only moves in a plane parallel to the surface of water (will not go above or below water (z-axis)) and turn only along the z axis (without tilting or tipping over). For a relatively stable surface craft, this turns out to be a safe assumption and helps simplify the boat model. It is also common to separate the analysis into two parts, namely the low frequency model (in 3D, described above) and a wave-frequency model which is generally added as an output disturbance.

While there are several ways to represent the coordinate system and associated nomenclature, we adopt the widely

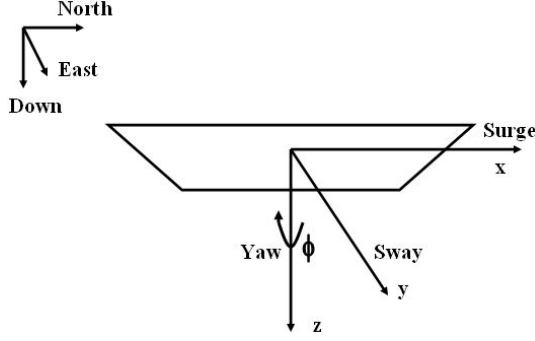


Fig. 4. Coordinate System used in Marine Navigation

used SNAME [17] notation:

$$\begin{aligned}\eta_1 &= [x, y, z]^T & \eta_2 &= [\phi, \theta, \psi]^T \\ \nu_1 &= [u, v, w]^T & \nu_2 &= [p, q, r]^T\end{aligned}$$

where  $\eta_1$  denotes the position vector in an earth-fixed frame,  $\eta_2$  is a vector of Euler angles,  $\nu_1$  denotes the body-fixed linear surge, sway and heave velocity vectors, and  $\nu_2$  denotes the body fixed angular roll, pitch and yaw velocity vectors.

Of the above, we only make use of the position vector  $\eta = [x, y, \psi]^T$  in the earth-fixed frame and the corresponding surge, sway and yaw velocity vectors  $\nu = [u, v, r]^T$  (shown in Figure 4).

This gives us the following 3 DOF kinematic system:

$$\dot{\eta} = \mathbf{R}(\psi)\nu \quad (1)$$

where

$$\mathbf{R}(\psi) = \mathbf{C}_{z,\psi}^T = \begin{bmatrix} c\psi & -s\psi & 0 \\ s\psi & c\psi & 0 \\ 0 & 0 & 1 \end{bmatrix}$$

The nonlinear 6 DOF equation for an aquatic vessel is given by:

$$\begin{aligned}\mathbf{M}\dot{\nu} + \mathbf{C}_{RB}(\nu)\nu + \mathbf{C}_A(\nu_r)\nu_r + \mathbf{D}(\nu_r) + \mathbf{G}(\eta) \\ = \tau_{env} + \tau_{thrust}\end{aligned}$$

where the left hand side consists of the inertial, coriolis, centripetal, damping and restoring forces (due to buoyancy and gravitation) respectively and the right hand side represents generalized external forces acting on the boat,  $\tau_{env}$  represents the environmental loads,  $\tau_{thrust}$  represents the thrust generated by the propulsion system.

For a slow moving surface vessel, we can ignore some of the terms from the general equation since they are small or not very relevant. Our boat moves at a slow speed and therefore the coriolis and centripetal forces are small. The damping forces are compensated in the thruster force term. The restoration force can be ignored for the surface craft assuming the buoyancy and gravitational forces balance each other to keep the boat afloat.

The low frequency motion model for the boat can be re-written as:

$$\mathbf{M}\dot{\nu} = \tau_{env} + \tau_{thrust} \quad (2)$$

where the system inertia matrix  $\mathbf{M}$  is given by:

$$\mathbf{M} = \begin{bmatrix} m - X_{\dot{u}} & 0 & 0 \\ 0 & m - Y_{\dot{v}} & mx_G - Y_{\dot{r}} \\ 0 & mx_G - Y_{\dot{r}} & I_z - N_{\dot{r}} \end{bmatrix} \quad (3)$$

where  $m$  is the vessel mass,  $I_z$  is the moment of inertia about the  $z$  axis.  $X_{\dot{u}}$ ,  $Y_{\dot{v}}$ ,  $Y_{\dot{r}}$ ,  $N_{\dot{v}}$ ,  $N_{\dot{r}}$  are the added mass coefficient terms due to accelerations along the corresponding and coupled axis determined using *strip theory* [18].  $(x_G, y_G, z_G)$  is the center of gravity.

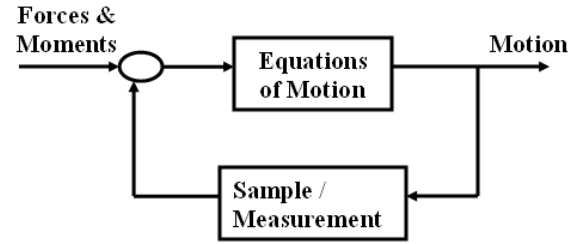


Fig. 5. Boat Motion Model for Maneuvering

Various models of ship steering have been proposed [4], [19]–[21]. We use a simplified model from [4]. We choose the origin to coincide with center of gravity.

Surge:

$$X = m(\dot{u} - vr)$$

Sway:

$$Y = m(\dot{v} + ur)$$

Yaw:

$$N = I_z \dot{r}$$

where  $X, Y$  are the external force vectors along the  $x$  (longitudinal) and  $y$  (transverse) axes respectively and  $N$  is the moment of external forces along the  $Z$  axis.

The thrust generated by the propeller is given by:

$$\tau_{thrust} = \rho_w D^4 K_T |n|n \quad (4)$$

where  $\rho_w$  is the air density,  $D$  is the propeller diameter, and  $n$  is the actual propeller speed (revolutions per second - rps).  $K_T$  is the strictly positive thrust coefficient where the effect of thrust losses has been accounted for and was determined experimentally by performing the tests in controlled environments.

Wind is generally modeled as a mean speed (slowly varying) with a fluctuating component incorporating wind gusts added as a noise term [22]. Let  $V_w$  and  $\beta_w$  represent the wind velocity and direction respectively. The components of wind velocity are:

$$u_w = V_w \cos(\beta_w - \psi) \quad v_w = V_w \sin(\beta_w - \psi) \quad (5)$$

and the relative wind velocity vector is given by:

$$\nu_{rw} = [u - u_w, v - v_w, r]^T$$

The total relative wind velocity is:

$$U_{rw} = \sqrt{(u - u_w)^2 + (v - v_w)^2} \quad (6)$$

The relative wind angle can be found by:

$$\gamma_w = \text{atan2}(-(v - v_w), -(u - u_w)) \quad (7)$$

The wind load vector is then given by:

$$\tau_{wind} = 0.5\rho_a \begin{bmatrix} \mathbf{A}_x \mathbf{C}_{wx}(\gamma_w) |\mathbf{U}_{rw}| \mathbf{U}_{rw} \\ \mathbf{A}_y \mathbf{C}_{wy}(\gamma_w) |\mathbf{U}_{rw}| \mathbf{U}_{rw} \\ \mathbf{A}_y \mathbf{L} \mathbf{C}_{w\psi}(\gamma_w) |\mathbf{U}_{rw}| \mathbf{U}_{rw} \end{bmatrix} \quad (8)$$

Here  $\rho_a$  is the density of air,  $\mathbf{L}$  is the overall length of the boat,  $\mathbf{A}_x$  and  $\mathbf{A}_y$  are the lateral and longitudinal areas of the non-submerged part of the boat projected on the xz-plane and yz-plane respectively,  $\mathbf{C}_{wx}(\gamma_w)$ ,  $\mathbf{C}_{wy}(\gamma_w)$  and  $\mathbf{C}_{w\psi}(\gamma_w)$  are the non-dimensional wind coefficients in surge, sway and yaw respectively. These are determined experimentally.

#### IV. LOCALIZATION

We implement an extended Kalman filter to which sensor inputs are provided as and when they arrive. The global positioning system (GPS) provides position measurements, the compass provides the heading (orientation) measurements and the wind sensors provide the measurements related to wind speed and direction. Each of the sensors has its own update rate and error characteristics. In the absence of any sensor measurements arriving, the filter proceeds by dead reckoning using the dynamic model of the boat. If some of the sensors are not available, the filter localizes the boat using the ones that are available.

The state vector consists of the position  $[x, y, \psi]$  and velocity  $[u, v, r]$  vectors in the 3 DOF discussed in Section III.

The system model is:

$$x_k = f(x_{k-1}, u_k) + \tau w_k; w_k \sim N(0, Q_k)$$

The measurement model is:

$$z_k = h(x_k) + v(k); v_k \sim N(0, R_k)$$

We start from a known fixed location and provide its information to the filter:

$$\hat{x}_0 = x_0; \hat{P}_0 = P_0$$

The filter operates in two phases. During the first phase (propagation phase), we propagate the state estimate and error covariance using the following equations:

$$\begin{aligned} \hat{x}_k^- &= f(\hat{x}_{k-1}, u_k) \\ P_k^- &= \phi_k P_{k-1} \phi_k^T + \tau_k Q_{k-1} \tau_k^T \end{aligned}$$

During the second phase (update phase), whenever we receive a measurement update, the gain matrix, state estimate and error covariance are updated using the following equations:

$$K_k = P_k^- H_k^T [H_k P_k^- H_k^T + R_k]^{-1}$$

$$\hat{x}_k = \hat{x}_k^- + K_k [z_k - h(\hat{x}_k^-)]$$

$$P_k = [I - K_k H_k] P_k^-$$

where

$$\phi_k = \partial f(\cdot) / \partial x_k |_{x_k = \hat{x}_k}$$

$$H_k = \partial h(\cdot) / \partial x_k |_{x_k = \hat{x}_k}$$

The filter was implemented offline and its performance was analyzed using data gathered from real boat experiments. These are described in Section VI.

#### V. CONTROL

In field experiments the boat can either be used in manual mode where the operator can specify the speed and heading of the boat via a joystick or in autonomous (waypoint following) mode where the operator uploads a sequence of GPS locations designating the path to be followed by the boat. Our waypoint following control is the commonly used *follow – the – carrot/goal* method. The navigation algorithm on the boat uses the current location estimate from the localization process and computes the distance to the next waypoint and the desired heading and generates the control commands for the boat (rudder angle and propeller speed) so as to minimize the heading and distance errors using PID control.

The PI control equation for propeller speed control is shown in Equation 9, where  $v_{cmd}$  is the command sent to the propeller control servo on the boat,  $v_{cur}$  is the current velocity,  $v_{des}$  is the desired velocity,  $K_p$  is the proportional gain and  $K_i$  is the integral gain. The gain terms were determined and tuned empirically based on experimental data.

$$v_{cmd} = K_p (v_{des} - v_{cur}) + K_i \int (v_{des} - v_{cur}) dt \quad (9)$$

The PID control equation for rudder angle control is shown in Equation 10, where  $\psi_{cmd}$  is the command sent to the rudder control servo on the boat,  $\psi_{des}$  is the desired heading,  $\psi_{cur}$  is the current heading,  $K_{phead}$  is the proportional gain,  $K_{dhead}$  is the derivative gain and  $K_{ihead}$  is the integral gain.

$$\begin{aligned} \psi_{cmd} &= K_{phead} (\psi_{des} - \psi_{cur}) + K_{dhead} (\dot{\psi}_{des} - \\ &\quad - \dot{\psi}_{cur}) + K_{ihead} \int (\psi_{des} - \psi_{cur}) dt \end{aligned} \quad (10)$$

## VI. EXPERIMENTS

### A. Localization Experiments

1) *Setup and Data Collection:* The data for the experiments was gathered by performing several runs spanning a set of target points with the robotic boat. A specified path was chosen for the boat and visual markers were placed at locations along this path. The exact location of these markers was surveyed using differential GPS to provide ground truth information and this was used for comparing the results we obtained. We did not use the raw GPS data for comparison of our results as it had large errors (between 7.5m and 11m).

The boat was made to move along the path under human guidance while the computer on the boat logged sensor measurements from the GPS, compass and also the control inputs sent to the motor controllers for the propeller and rudder. All the gathered data was time-stamped for offline analysis.

Due to the limited payload capacity of the boat, we could not mount the wind sensors on the boat. We made the assumption that wind conditions (direction and speed) in a small open region on the surface of the lake are homogeneous. This simplified the data gathering since it allowed us to gather wind direction and speed data by placing a weather station buoy along the actual path of the boat (rather than on the boat itself). We validated our assumption of homogeneity by comparing the wind data reported by the weather buoy at points close to the start and end of the path taken by the boat. The clock on the boat and weather station were synchronized at the start of the experiment.

2) *Data Processing:* Typical position accuracy achievable by Garmin 16A GPS is less than 15m with a 95% confidence level (See Table I). Depending on the location of the experiment, we obtained accuracies between 7.5m and 11m. The need for better localization warrants us to use an extended Kalman filter.

We use the model we developed in Section III. The measurements from the GPS, compass and wind sensors were made available to the extended Kalman filter at the same rate and in the same order in which they were gathered and were used in the update phase of the filter.

The measurements from all the sensors do not arrive simultaneously. They are processed in the order of arrival. To handle the problem of missing sensor measurements during the update phase, the corresponding columns in the  $H$  matrix are set to zero for the missing measurements.

The GPS measurements provide the position of the boat (latitude and longitude) in the earth-fixed frame which are converted to northing's and easting's and provided to the filter to update the estimate of the position of the boat  $(x, y)$ .

The compass measurements provide the heading of the boat relative to the Earth's geographic north. These measurements are provided to the filter to update the estimate of the orientation of the boat  $(\psi)$ .

The wind direction and speed measurements are provided to the filter to update its estimate of the surge and sway velocities  $(u, v)$ .

TABLE II  
FILTER INPUTS VS. ACCURACY (ECHO PARK)

Control Inputs	Measurement Inputs	Error @40m	Error @100m	Error @160m
Yes	None	28.14m	69.52m	117.57m
Yes	Compass	7.98m	13.68m	19.63m
Yes	Compass Wind	4.23m	4.39m	6.31m
Yes	Compass GPS	1.67m	1.41m	2.80m

$$z_1 = x_{gps} + v_1 \quad (\text{surge-position})$$

$$z_2 = y_{gps} + v_2 \quad (\text{sway-position})$$

$$z_3 = \psi_{compass} + v_3 \quad (\text{yaw-angle})$$

$$z_4 = V_w + v_4 \quad (\text{wind-speed})$$

$$z_5 = \beta_w + v_5 \quad (\text{wind-direction})$$

where the measurement noise  $v_i$  ( $i=1..5$ ) is modeled as zero-mean Gaussian white noise.

We did not have measurements available to update the velocity vector  $(u, v, r)$ . These were in turn determined based on the control inputs that were provided to the boat. We determined the conversion parameters for different commanded inputs into equivalent thruster force and conversion efficiency parameters needed to determine the boat speed using the Straight-Line Test [5]. We also determined the turn rate characteristic and its coupling to the boat speed and rudder angle by carrying out these tests in still water.

3) *Results:* We had two goals in mind while performing these tests. We wanted to determine the performance of the filter in the presence of selected sensors being available. To analyze this, the same measurement set was used but different sensor measurement combinations were provided to the filter. The combinations we tried and the corresponding results for our two field sites are summarized in Tables II, III. The results presented in these tables are average values from 10 runs each over the same path. The data obtained from differential GPS was used as ground truth for these experiments. In the table an average error of 1.67m at 40m from the start location using compass and GPS sensor as input means that the location estimate from the extended Kalman filter was off by about 1.67m from the DGPS reported location (available ground truth). Figures 6, 7 show visualizations depicting the predicted trajectory by the state estimator in the presence of control inputs and different sensor measurements.

Our results indicate that a very accurate dynamic system model is not required to perform good localization given the availability of a few sensors. Availability of a relatively simple sensor like a compass which can provide heading measurements can greatly help in providing good localization. The availability of more sensor measurements of various kinds (wind measurements, GPS etc.) helps improve the localization accuracy significantly. The results indicate that in the absence of any measurement data, we need a very effective model of the boat to be able to localize it.

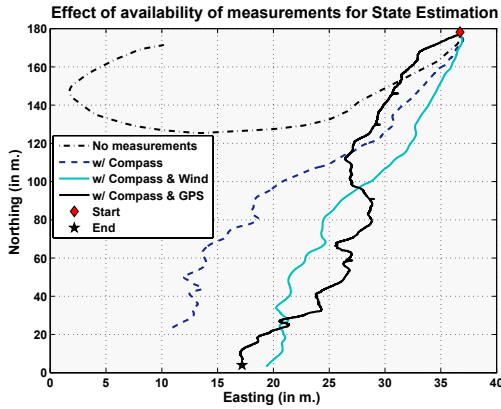


Fig. 6. Result of localization on Echo Park data

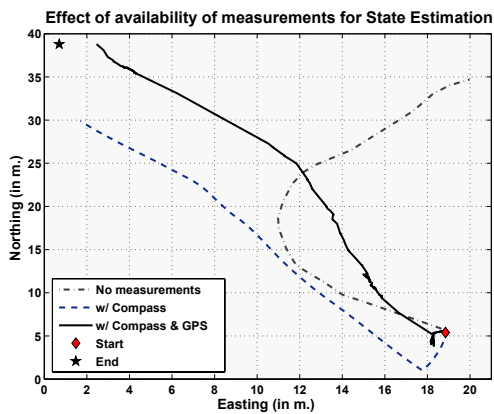


Fig. 7. Result of localization on James Reserve data

### B. Autonomous Navigation Experiments

We performed fifteen field tests with the boat to evaluate its navigation performance. Our experiments were performed at Lake Fulmor, James Reserve, CA and Echo Park Lake in Los Angeles, CA.

The boat was provided with a set of waypoints to be traversed in the given order. A GPS and compass were available on the boat to provide position and heading measurements. Wind measurements were not available during these experiments. The algorithm running on the boat used the measurements provided by the GPS and compass to compute the control commands for the propeller and the rudder.

Figures 8, 9 show results from our autonomous runs with the boat. The scale along x-axis for Figure 9 has been scaled to give the reader a better feel for typical accuracies achievable in the field by the GPS. The results indicate that the boat follows the specified path (in terms of GPS way-points) closely and reaches the specified target locations within the specified acceptable range. Typical GPS accuracy achieved during these runs was between 7.5m and 11m (Note that the errors are similar irrespective of the direction of travel of the boat, i.e., going between north and south vs.

TABLE III  
FILTER INPUTS VS. ACCURACY (JAMES RESERVE)

Control Inputs	Measurement Inputs	Error @35m	Error @55m	Error @93m
Yes	None	33.76m	43.62m	46.88m
Yes	Compass	9.64m	16.32m	18.07m
Yes	Compass Wind	7.63m	12.34m	14.32m
Yes	Compass GPS	2.07m	2.19m	2.11m

east and west).

The results demonstrate the very high dependence on position measurements from GPS. This can be observed by comparing the results presented in Figures 8, 9. Better GPS measurements were available at the Echo Park site compared to the James Reserve site.

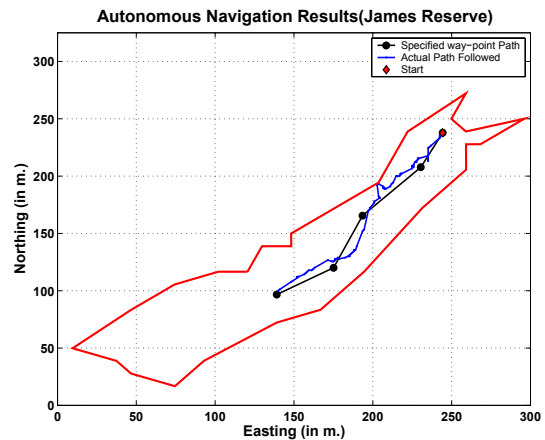


Fig. 8. Result of autonomous navigation at James Reserve, CA

## VII. CONCLUSIONS AND FUTURE WORK

We described a dynamic model of a robotic boat, an algorithm for estimating its location by integrating sensor inputs, a controller for waypoint following and extensive field experiments (over 10 km aggregate) to validate each of these. We tested the localization accuracy in different sensing regimes as a prelude to accommodating sensing failures.

We are in the process of refining our boat model, as well as implementing a framework for fault detection and recovery as a prelude to using the boat as part of a measurement campaign in the field.

## VIII. ACKNOWLEDGEMENTS

The authors thank David Caron, Arvind Pereira, Steffi Moorthi, Carl Oberg, and Beth Stauffer for their comments and help with the experiments. This work is supported by the National Science Foundation under grant CCF-0120778.

## REFERENCES

- [1] D. A. Caron, "Marine microbial ecology in a molecular world: what does the future hold?" *Scientia Marina*, no. 69, pp. 97–110 Suppl. 1, 2005.

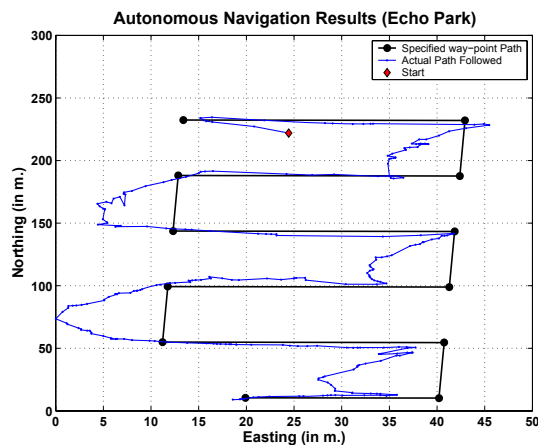


Fig. 9. Result of autonomous navigation at Echo Park

- [2] A. Dhariwal, B. Zhang, B. Stauffer, C. Oberg, G. S. Sukhatme, D. A. Caron, and A. A. Requicha, "Networked aquatic microbial observing system," in *IEEE International Conference on Robotics and Automation*. Orlando, FL: IEEE, May 2006, pp. 4285–4287.
- [3] G. S. Sukhatme, A. Dhariwal, B. Zhang, C. Oberg, B. Stauffer, and D. A. Caron, "The design and development of a wireless robotic networked aquatic microbial observing system," *Environmental Engineering Science*, 2006.
- [4] T. Fossen, *Marine Control Systems: Guidance, Navigation and Control of Ships, Rigs and Underwater Vehicles*. Marine Cybernetics AS, Trondheim. ISBN 82-92356-00-2, 2002, 1st. Ed., 3rd. Printing, 586 pages.
- [5] T. Perez, T. I. Fossen, and A. J. Sorensen, "A discussion about seakeeping and manoeuvring models for surface vessels," NTNU, TechReport MSS-TR-001, 2004.
- [6] J. Ebken, M. Bruch, and J. Lum, "Applying unmanned ground vehicle technologies to unmanned surface vehicles," 2005, Space and Naval Warfare Systems Center, San Diego, CA.
- [7] A. Kelly, "A 3d space formulation of a navigation kalman filter for autonomous vehicles," Robotics Institute, Carnegie Mellon University, Pittsburgh, PA, Tech. Rep. CMU-RI-TR-94-19, May 1994.
- [8] G. Dissanayake, P. Newman, H. F. Durrant-Whyte, S. Clark, and M. Csorba, "A solution to the simultaneous localization and map building (slam) problem," *IEEE Trans. on Robotics and Automation*, no. 17(3), pp. 229–241, 2001.
- [9] S. Thrun, D. Fox, and W. Burgard, "A probabilistic approach to concurrent mapping and localization for mobile robots," *Machine Learning*, vol. 31, pp. 29–53, 1998, also appeared in *Autonomous Robots* 5, 253–271 (joint issue).
- [10] J. J. Leonard and H. F. Durrant-Whyte, "Simultaneous map building and localization for an autonomous mobile robot," in *IEEE Int. Workshop on Intelligent Robots and Systems*, Osaka, Japan, Nov 1991, pp. 1442–1447, also presented at the 2nd IARP Int. Conf. on Multi-Sensor Fusion and Environment Modelling, Oxford, UK, September 1991.
- [11] F. Lu and E. Miliotis, "Robot pose estimation in unknown environments by matching 2d range scans," in *CVPR94*, 1994, pp. 935–938.
- [12] S. Saripalli, J. M. Roberts, P. I. Corke, G. Buskey, and G. S. Sukhatme, "A tale of two helicopters," in *IEEE/RSJ International Conference on Intelligent Robots and Systems*, Oct 2003, pp. 805–810.
- [13] R. van der Merwe and E. Wan, "Sigma-point kalman filters for integrated navigation," in *Proceedings of the 60th Annual Meeting of The Institute of Navigation (ION)*, Dayton, OH, June 2004. [Online]. Available: <http://cslu.cse.ogi.edu/publications/ps/merwe04a.pdf>
- [14] M. Benjamin, J. Curcio, J. Leonard, and P. Newman, "Navigation of unmanned marine vehicles in accordance with the rules of the road," in *IEEE International Conference on Robotics and Automation*, May 2006.
- [15] S. B. Williams, P. Newman, M. W. M. G. Dissanayake, and H. Durrant-Whyte, "Autonomous underwater simultaneous localisation and map building," in *IEEE International Conference on Robotics and Automation*, San Francisco, CA, USA, Apr 2000.
- [16] A. J. Sorensen, *Marine Cybernetics: Modelling and Control*. Lecture Notes, Fifth Edition, UK-05-76, Department of Marine Technology, the Norwegian University of Science and Technology, Trondheim, Norway, 2005.
- [17] *Nomenclature for Treating the Motion of a Submerged Body Through a Fluid*. SNAME. The Society of Naval Architects and Marine Engineers, 1950, no. 1-5.
- [18] C. J.P., *Principles of naval architecture*. New York: The Society of Naval Architects and Marine Engineers, 1967.
- [19] K. Davidson and L. Schiff, "Turning and course keeping qualities," *Transactions of SNAME*, vol. 54, 1946.
- [20] K. Nomoto, T. Taguchi, K. Honda, and S. Hirano, "On the steering qualities of ships," *International Shipbuilding Progress*, Tech. Rep., 1957, vol. 4.
- [21] A. A. Gelb, *Applied Optimal Estimation*. Cambridge, MA: MIT Press, 1974.
- [22] M. Isherwood, "Wind resistance of merchant ships," *Transactions of the Royal Institution of Naval Architects*, vol. 115, pp. 327–338, 1972.